Supporting Information: Photoisomerization transition state manipulation by entangled two-photon absorption

Bing Gu,[1,*] Daniel Keefer,[1,*] Flavia Aleotti,[2] Artur Nenov,[2] Marco Garavelli,[2] and Shaul Mukamel[1,†]

[1] *Department of Chemistry and Department of Physics & Astronomy, University of California, Irvine, California, 92697, USA*

[2] *Dipartimento di Chimica Industriale "Toso Montanari", Università degli studi di Bologna, Viale del Risorgimento 4, 40136 Bologna, Italy.*

* These two authors contributed equally

† smukamel@uci.edu

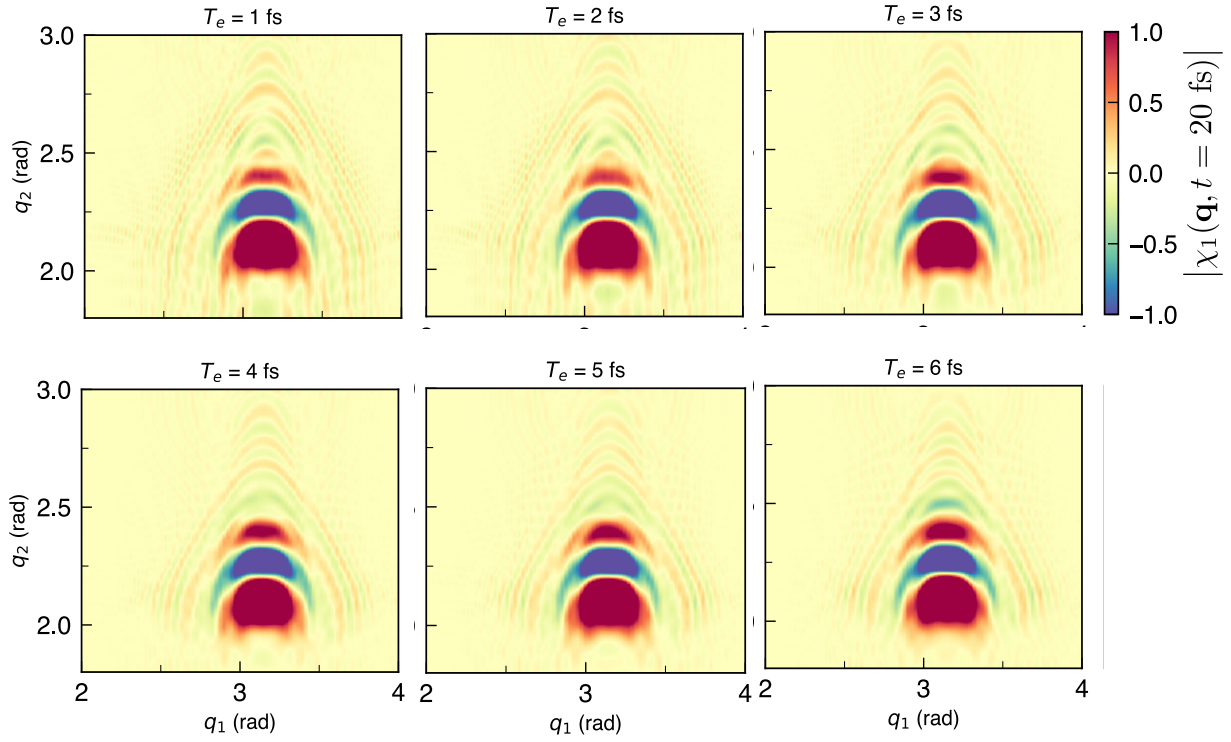

FIG. S1. Same as Fig. 5 in the main text but with classical pulses with long frequency tails.

S1. DERIVATION OF ETPA SIGNAL (EQ. (2))

The full field-molecular system is described by the molecular quantum electrodynamical Hamiltonian in the electric-dipole approximation

$$H = H_{\mathrm{M}} + H_{\mathrm{R}} + H_{\mathrm{RM}}, \quad H_{\mathrm{M}} = T_{\mathrm{n}} + H_{\mathrm{BO}}(\mathbf{q}) \tag{S1}$$

where H_{M} is the molecular Hamiltonian with T_{n} the nuclear kinetic energy operator and $H_{\mathrm{BO}}(\mathbf{q}) = \sum_\alpha V_\alpha(\mathbf{q}) \left|\psi_\alpha(\mathbf{q})\right\rangle \left\langle\psi_\alpha(\mathbf{q})\right|$ the Born-Oppenheimer Hamiltonian with $V_\alpha(\mathbf{q})$ the αth adiabatic potential energy surface and $|\psi_\alpha(\mathbf{q})\rangle$ the adiabatic electronic state, $H_{\mathrm{R}} = \sum_{i=1}^{2} \int_0^\infty \hbar\omega \left(a_i^\dagger(\omega) a_i(\omega) + \frac{1}{2}\right) \mathrm{d}\omega$ describes the signal and idler beams generated in e.g. the SPDC process, $H_{\mathrm{RM}} = \sum_j -\boldsymbol{\mu}(\mathbf{q}) \cdot \hat{\mathbf{E}}_j(\mathbf{r}_0)$ is the electric-dipole coupling with

$$\hat{\mathbf{E}}_j^{(+)}(\mathbf{r}_0) = i \int_0^\infty \mathrm{d}\omega \mathcal{E}(\omega) \mathbf{e}_j a_j(\omega) e^{-i\mathbf{k}\cdot\mathbf{r}_0} \tag{S2}$$

the positive-frequency component of the electric field operator of jth photon beam at molecular location $\mathbf{r}_0$, and $\mathcal{E}(\omega) \equiv \sqrt{\frac{\hbar\omega}{2\epsilon_0 V}}$ is the single-photon electric field. The joint electron-nucleus-photonic space is given by the tensor product of the electron-nuclear Hilbert space and the Fock space of photon modes

$$|\Psi\rangle = \sum_{\alpha,\mathbf{n}} |\psi_\alpha(\mathbf{q})\rangle \, |\chi_{\alpha,\mathbf{n}}(t)\rangle \, |n(\omega)\cdots\rangle \tag{S3}$$

where $\chi_{\alpha,\mathbf{n}}(\mathbf{q}, t)$ the nuclear wavefunction at αth electronic state and photon state $|\mathbf{n}\rangle$, $|\mathbf{n}\rangle \equiv |n(\omega)n(\omega')\cdots\rangle$ describes the photon state in the occupation number representation.

The initial state of the joint light-matter system is $|\psi_0(\mathbf{q})\rangle \, |\chi_0\rangle \, |\Phi_0\rangle$ where $|\Phi_0\rangle$ describes the quantum light. In the interaction picture of $H_0 = H_{\mathrm{M}} + H_{\mathrm{R}}$, the global state at time t can be derived using the time-dependent perturbation theory (see Sec. S1)

$$|\Psi_I(t)\rangle = |\Psi_0\rangle - \left(\int_{t_0}^{t} \mathrm{d}t_2 \int_{t_0}^{t_2} \mathrm{d}t_1 \mu_{\mathrm{i}}(t_2) \mu_{\mathrm{s}}(t_1) \, |\psi_0(\mathbf{q})\rangle \, |\chi_0\rangle \, E_{\mathrm{i}}^{(+)}(t_2) E_{\mathrm{s}}^{(+)}(t_1) \, |\Phi_0\rangle + (\mathrm{s} \leftrightarrow \mathrm{i}) \right) \tag{S4}$$

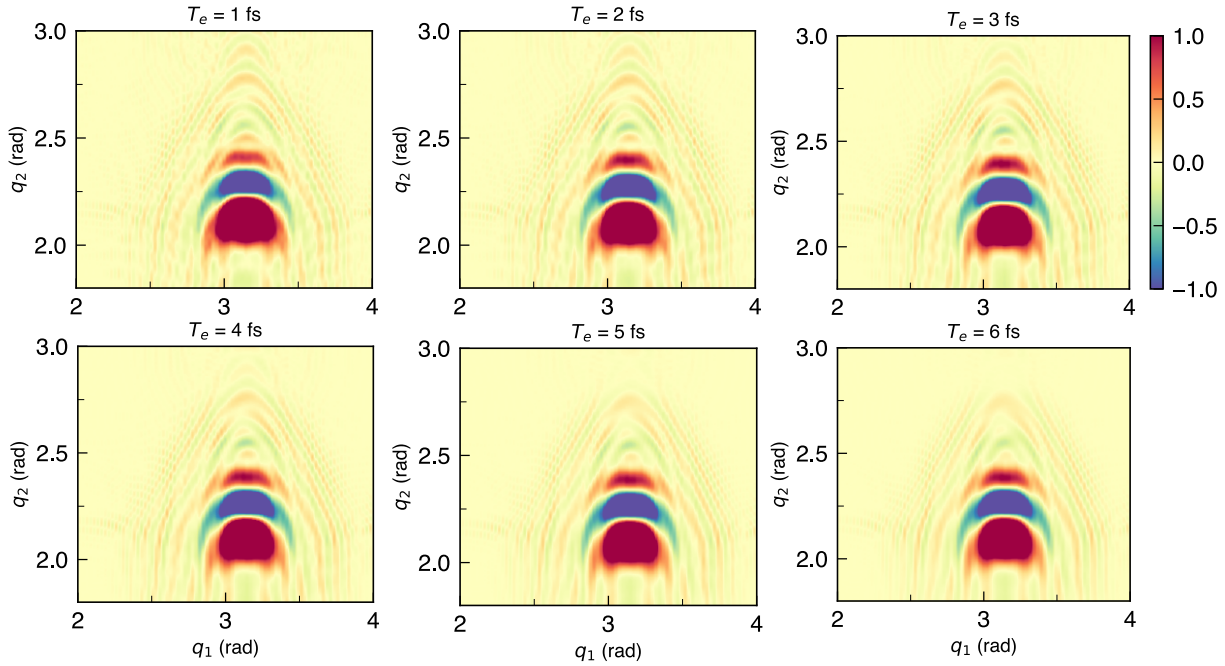

FIG. S2. Classical two-photon excited nuclear wavepackets in the S_1 surface at $t = 20$ fs with linearly chirped Gaussian pulses. The bandwidth is varied in correspondence to different entanglement times T_e used in Fig. 5 (indicated). The excited wavepackets shows negligible dependence on the bandwidth.

where $\mu_j = \boldsymbol{\mu} \cdot \mathbf{e}_j$. Since the photons are off-resonant with molecular transitions, the one-photon processes are neglected in Eq. (S4). Using Eq. (S4) to calculate the population of the final products $\mathcal{P}(t) = \langle \Psi(t)|\mathcal{P}|\Psi(t)\rangle$ then yields Eq. (3) in the main text.

S2. TWO-PHOTON TRANSITION AMPLITUDE

The two-photon detection amplitude can be obtained from the JSA

$$A(t_2, t_1) \equiv \langle 0|E^{(+)}(t_2)E^{(+)}(t_1)|\Phi\rangle \tag{S5}$$

where the electric field operator can be approximated by

$$E_j(t) \approx ie^{-i\bar{\omega}_j t}\mathcal{E}(\bar{\omega}_j)\int_{-\infty}^{+\infty} \mathrm{d}\Delta_j a_j(\bar{\omega}_j + \Delta_j)e^{-i\Delta_j t} \tag{S6}$$

with $a(\omega)$ the boson annihilation operator satisfying $\left[a(\omega), a^\dagger(\omega')\right] = \delta(\omega - \omega')$. Using Eq. (S6), the two-photon transition amplitude leads to

$$\begin{aligned} A_{21}(t, t') &= \exp\left(-i\bar{\omega}_1 t' - i\bar{\omega}_2 t\right)\mathcal{E}(\bar{\omega}_1)\mathcal{E}(\bar{\omega}_2)\iint_{-\infty}^{\infty} \mathrm{d}\Delta_1\,\mathrm{d}\Delta_2 f(\Delta_1, \Delta_2)e^{-i\Delta_1 t' - i\Delta_2 t} \\ &= \exp\left(-i\bar{\omega}_1 t' - i\bar{\omega}_2 t\right)\mathcal{E}(\bar{\omega}_1)\mathcal{E}(\bar{\omega}_2)f(t', t) \end{aligned} \tag{S7}$$

where $\bar{\omega}_j$ is the central frequency of j-th beam, and $\Delta_j = \omega_j - \bar{\omega}_j$, $f(t, t')$ is the joint temporal amplitude (i.e., double Fourier transform of the JSA).

S3. WAVEPACKET PROPAGATION

The effective Hamiltonian describing the coupled electron-nuclear dynamics, in the space of the two nuclear coordinates q_1 and q_2, is given by

$$\hat{H} = \begin{pmatrix} \hat{T} + \hat{V}_g(\mathbf{q}) & -\varepsilon(t)\hat{\mu}_{eg}(\mathbf{q}) + \hat{K}_{ge} \\ -\varepsilon(t)\hat{\mu}_{eg}(\mathbf{q}) - \hat{K}_{eg} & \hat{T} + \hat{V}_e(\mathbf{q}) \end{pmatrix}. \tag{S8}$$

The potential energy surfaces $\hat{V}(\mathbf{q})$ of the participating electronic states (Fig. 3) were computed using high–level RASPT2 with an active space of 18 electrons in 16 orbitals (all π and π^* orbitals and two nitrogen n-orbitals). The MOLCAS8 program package [1] with the ANO-L-VDZP basis set [2] was employed. The surfaces were discretized on a numerical grid with 1024 points in CNNC and 512 in the symmetric CNN bending.

The kinetic energy operator $\hat{T}$ in Eq. S8 in the G–Matrix formalism is given by [3, 4]

$$\hat{T} \simeq -\frac{\hbar^2}{2m} \sum_{o=1}^{2} \sum_{p=1}^{2} \frac{\partial}{\partial q_o} \left[G_{op} \frac{\partial}{\partial q_p} \right] \tag{S9}$$

with $o, p \in \mathbf{q}$ and the G-Matrix computed via its inverse elements

$$\left(G^{-1}\right)_{op} = \sum_{i=1}^{3N} m_i \frac{\partial x_i}{\partial q_o} \frac{\partial x_i}{\partial q_p} \quad . \tag{S10}$$

$\hat{K}_{ge}$ in Eq. S8 approximates the non–adiabatic couplings and is given by[5]

$$\hat{K}_{ge} = \frac{1}{2m} \left(2 f_{ge} \frac{\partial}{\partial \mathbf{q}} + \frac{\partial}{\partial \mathbf{q}} f_{ge} \right) \tag{S11}$$

and f_{ge} contains terms $\langle \psi_g | \, \frac{\partial}{\partial \mathbf{q}} \psi_e \rangle$ with the electronic wavefunction $\psi(\mathbf{r}; \mathbf{q})$.

The starting nuclear wavefunction $\chi(\mathbf{q}, t = 20fs)$ is obtained by entangled two-photon absorption of the S_0 ground state vibrational wavefunction $\chi_0(\mathbf{q})$ by Eq. (3). $\chi(\mathbf{q}, t = 20fs)$ was then propagated using a Chebychev scheme [6] with a time step of 0.05 fs starting from $t_0 = -20$ fs. Periodic boundary conditions were employed along CNNC in S_1 while in S_0 a Butterworth filter [7] absorbs the wavepacket at CNNC = 0° and 360°.

S4. NON-REACTIVE CONICAL INTERSECTION SEAM

[1] Francesco Aquilante, Jochen Autschbach, Rebecca K. Carlson, Liviu F. Chibotaru, Mickaël G. Delcey, Luca De Vico, Ignacio Fdez. Galván, Nicolas Ferré, Luis Manuel Frutos, Laura Gagliardi, Marco Garavelli, Angelo Giussani, Chad E. Hoyer, Giovanni Li Manni, Hans Lischka, Dongxia Ma, Per Åke Malmqvist, Thomas Müller, Artur Nenov, Massimo Olivucci, Thomas Bondo Pedersen, Daoling Peng, Felix Plasser, Ben Pritchard, Markus Reiher, Ivan Rivalta, Igor Schapiro, Javier Segarra-Martí, Michael Stenrup, Donald G. Truhlar, Liviu Ungur, Alessio Valentini, Steven Vancoillie, Valera Veryazov, Victor P. Vysotskiy, Oliver Weingart, Felipe Zapata, and Roland Lindh, "Molcas8: New capabilities for multiconfigurational quantum chemical calculations across the periodic table," Journal of Computational Chemistry **37**, 506–541 (2016).

[2] Per-Olof Widmark, P.-A. Malmqvist, and B. O. Roos, "Density matrix averaged atomic natural orbital (ANO) basis sets for correlated molecular wave functions," Theoretica Chimica Acta **77**, 291–306 (1990).

[3] Peter H. Berens and Kent R. Wilson, "Molecular dynamics and spectra. I. Diatomic rotation and vibration," The Journal of Chemical Physics **74**, 4872–4882 (1981).

[4] Sebastian Thallmair, Matthias K. Roos, and Regina de Vivie-Riedle, "Design of specially adapted reactive coordinates to economically compute potential and kinetic energy operators including geometry relaxation," The Journal of Chemical Physics **144**, 234104 (2016).

[5] Sebastian Reiter, Daniel Keefer, and Regina de Vivie-Riedle, "Exact Quantum Dynamics (Wave Packets) in Reduced Dimensionality," in *Quantum Chemistry and Dynamics of Excited States* (John Wiley & Sons, Ltd, 2020) Chap. 11, pp. 355–381.

[6] H. Tal-Ezer and R. Kosloff, "An accurate and efficient scheme for propagating the time dependent Schrödinger equation," The Journal of Chemical Physics **81**, 3967–3971 (1984).

[7] Stephen Butterworth, "On the Theory of Filter Amplifiers," Experimental Wireless and the Wireless Engineer **7**, 536–541 (1930).

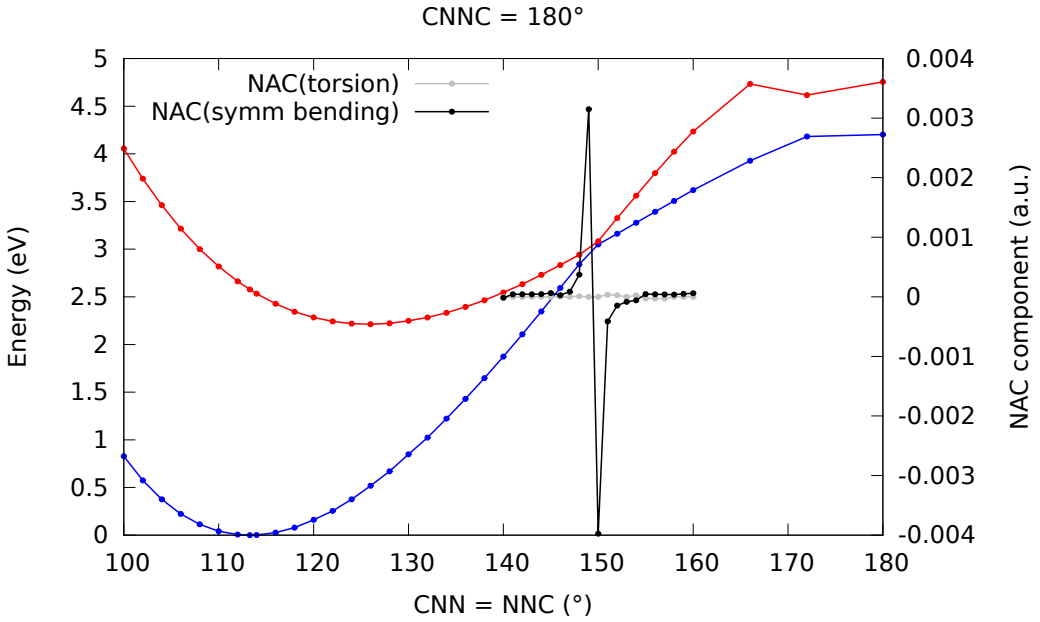

FIG. S3. Non-adiabatic coupling along the CNN symmetric bending angle with the CNNC torsion fixed at 180°. It is strong with respect to CNN and almost vanishing with respect to CNNC. The electronic wavefunction exhibits strong mixing at the energetic crossings for other CNNC values as well. We thus replicate the non-adiabatic coupling shown here along the CNNC torsion and shift it to the CNN angle exhibiting the minimal energy difference between S_1 and S_0. This yields the non-reactive non-adiabatic coupling seam depicted in Fig. 3.